

See discussions, stats, and author profiles for this publication at: <https://www.researchgate.net/publication/262993659>

# Synthesis of Sulfonic Acid-Containing Polybenzoxazine for Proton Exchange Membrane in Direct Methanol Fuel Cells

ARTICLE in MACROMOLECULES · JANUARY 2014

Impact Factor: 5.8 · DOI: 10.1021/ma4020214

CITATIONS

8

READS

73

8 AUTHORS, INCLUDING:



**Xiuling Yan**

Shandong University

15 PUBLICATIONS 260 CITATIONS

SEE PROFILE



**Zaijun Lu**

Shandong University

32 PUBLICATIONS 305 CITATIONS

SEE PROFILE



**Hatsuo Ishida**

Case Western Reserve University

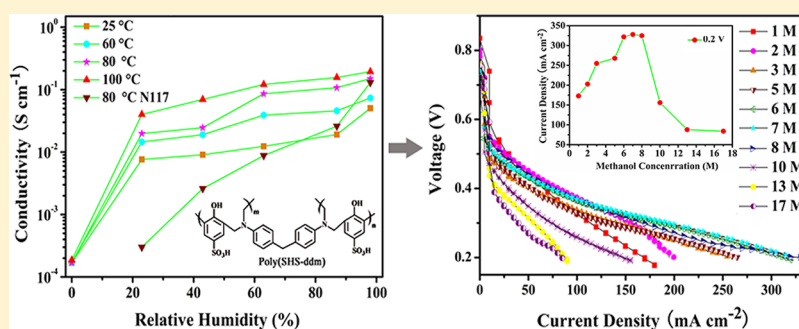
448 PUBLICATIONS 12,896 CITATIONS

SEE PROFILE

## Synthesis of Sulfonic Acid-Containing Polybenzoxazine for Proton Exchange Membrane in Direct Methanol Fuel Cells

Bingjian Yao,<sup>†</sup> Xiuling Yan,<sup>†</sup> Yi Ding,<sup>†</sup> Zaijun Lu,<sup>\*,†</sup> Daxuan Dong,<sup>‡</sup> Hatsuo Ishida,<sup>‡</sup> Morton Litt,<sup>‡</sup> and Lei Zhu<sup>\*,‡</sup><sup>†</sup>Key Laboratory of Special Functional Aggregated Materials, Ministry of Education, School of Chemistry and Chemical Engineering, Shandong University, Jinan 250100, P. R. China<sup>‡</sup>Department of Macromolecular Science and Engineering, Case Western Reserve University, Cleveland, Ohio 44106-7202, United States

## S Supporting Information



**ABSTRACT:** A novel sulfonic acid-containing benzoxazine monomer, 3-[4-(4-(6-sulfo-3,4-dihydro-2H-1,3-benzoxazine-3-yl)benzyl)phenyl]-3,4-dihydro-2H-1,3-benzoxazine-6-sulfonic acid (abbreviated as SHS-ddm), was synthesized via Mannich reaction and acidizing reaction using sodium 4-hydroxybenzenesulfonate, 4,4'-diaminodiphenylmethane, and paraformaldehyde as raw materials. The structure of SHS-ddm was characterized by Fourier transform infrared (FTIR) spectroscopy, proton nuclear magnetic resonance (<sup>1</sup>H NMR) spectroscopy, and electrospray ionization mass spectrometry (ESI-MS). The cross-linked sulfonic acid-containing polybenzoxazine [poly(SHS-ddm)] membrane was prepared through high temperature solution-casting method. Membrane properties including proton conductivity, methanol permeability, mechanical property, hydrolytic and oxidative stabilities were evaluated in detail. Our results showed that poly(SHS-ddm) membrane exhibited a high proton conductivity of 0.154 S cm<sup>-1</sup> at 80 °C and a very low methanol permeability of 5.8 × 10<sup>-8</sup> cm<sup>2</sup> s<sup>-1</sup>. The calculated selectivity parameter was 2.655 × 10<sup>6</sup> S s cm<sup>-3</sup>, which was much higher than that of Nafion 117 (8.081 × 10<sup>4</sup> S s cm<sup>-3</sup>). Employing this membrane in the membrane-electrode assembly (MEA), high methanol concentration up to 7 M was used. The cell exhibited a stable open circuit voltage (*V*<sub>OC</sub>) of 0.76 V and a maximum power density of 66.5 mW cm<sup>-2</sup>. Accordingly, only relatively low voltage drop of 1.415 mV h<sup>-1</sup> was observed after a continuous operation for 12 h. Overall, this novel polybenzoxazine exhibited special potential for proton exchange membrane with low methanol permeability and low cost in direct methanol fuel cells.

## INTRODUCTION

Proton exchange membranes (PEMs) are key components of polymer fuel cells because they can provide an ionic pathway for proton transfer while prevent the mixing of reactant gases. The most widely used PEM is Nafion membrane commercially available from DuPont. Nafion is the state-of-the-art material due to its high proton conductivity, good chemical and thermal stability.<sup>1–3</sup> However, further application of Nafion is hindered by the strong temperature dependence of its proton conductivity, high cost, and high methanol crossover rate for direct methanol fuel cells (DMFCs).<sup>4,5</sup> Two methods have been developed to overcome these problems. One is modification of Nafion.<sup>6</sup> The other is searching for alternative proton conducting materials, such as polyimides,<sup>7–9</sup> polybenzimidazoles,<sup>10–12</sup> and poly(arylene ether sulfone).<sup>13–16</sup>

Although these polymers exhibit excellent thermal stability, the chemical/electrochemical stability, dimensional stability, methanol selectivity, and proton conductivity still need to be improved.

Polybenzoxazine is a novel thermosetting resin with excellent properties, including good thermal stability, chemical resistance, and low cost.<sup>17–19</sup> Recently, polybenzoxazine-based PEMs were explored preliminarily. One approach used different benzoxazine monomers in a benzoxazine–benzimidazole copolymer, such as phosphorus-containing benzoxazine,<sup>20</sup> naphthoxazine benzoxazine,<sup>21</sup> fluorine-containing benzoxazine,<sup>22,23</sup> and 3-

Received: September 30, 2013

Revised: January 10, 2014

Published: January 21, 2014

phenyl-3,4-dihydro-6-*tert*-butyl-2*H*-1,3-benzoxazine.<sup>24</sup> The other approach used a sulfonic acid containing benzoxazine (SBa) cross-linker in sulfonated polyether ether ketone (SPEEK), where the functional sulfonic acid group was introduced by ester linkage.<sup>25</sup>

In spite of the success of benzoxazine-based copolymer, sulfonated polybenzoxazine homopolymer using as a host PEM material has not been reported so far. Moreover, the highly cross-linked network structures of polybenzoxazine homopolymer become an effective hindrance to the crossover of methanol molecules and make it possible to use high methanol concentration. Herein, we describe the synthesis and performance of a novel sulfonic acid-containing polybenzoxazine for PEM. Specifically, sodium 4-hydroxybenzenesulfonate, paraformaldehyde, and 4,4'-diaminodiphenylmethane are used as raw materials to synthesize the sulfonic acid containing benzoxazine via Mannich reaction. Polybenzoxazine was obtained through ring-opening polymerization at elevated temperatures. A direct connection between sulfonic acid group and benzene ring is expected to improve the hydrolytic stability. One sulfonic acid group in each repeating unit of polybenzoxazines is expected to improve proton conductivity. The cross-linked structure of polybenzoxazines contributes to the low methanol permeability and good dimensional stability. Furthermore, the low-cost raw materials will effectively reduce the synthetic cost of PEM materials.

## ■ EXPERIMENTAL SECTION

**Materials.** Sodium 4-hydroxybenzenesulfonate was purchased from Gracia Chemical Technology Co., Ltd. (Chengdu, China). Paraformaldehyde was purchased from Tianjin Kermel Chemical Reagent Co., Ltd. (Tianjin, China). 4,4'-Diaminodiphenylmethane from Shanghai Sanya Chemical Reagent Company (Shanghai, China) was recrystallized from ethanol. All solvents were of analytical grade and used as received.

**Synthesis of Sodium 3-[4-(4-(6-Sulfonato-3,4-dihydro-2*H*-1,3-benzoxazine-3-yl)benzyl)phenyl]-3,4-dihydro-2*H*-1,3-benzoxazine-6-sulfonate (SHS-ddm<sup>−</sup>Na<sup>+</sup>).** To a 100 mL three-necked flask were added 1.238 g (6.25 mmol) of 4,4'-diaminodiphenylmethane, 0.750 g (25 mmol) of paraformaldehyde, and 25 mL of dimethyl sulfoxide (DMSO). After the mixture was stirred for 0.5 h at room temperature, 2.450 g (12.5 mmol) of sodium 4-hydroxybenzenesulfonate was added into the reaction system. The mixture was maintained at 90 °C for 4 h. Upon cooling, the resulting mixture was precipitated in excess ethanol. The residue was subsequently recrystallized in ethanol to afford a white powder product in 80% yield. ESI-MS: calcd for C<sub>29</sub>H<sub>26</sub>N<sub>2</sub>O<sub>8</sub>S<sub>2</sub> M<sup>+</sup>, *m/z* 594.11; found, *m/z* 594.07 (S1). <sup>1</sup>H NMR (D<sub>2</sub>O, 300 MHz, ppm): 6.89–7.62 (14H, m, Ar-H), 5.38 (4H, s, −O−CH<sub>2</sub>−N−), 4.41 (4H, s, Ar−CH<sub>2</sub>−N), 3.65 (2H, s, Ar−CH<sub>2</sub>−Ar). FTIR (KBr, cm<sup>−1</sup>): 1228, 1035 (stretch, C−O−C); 2960, 2853, 1452 (CH<sub>2</sub>), 1599, 1498 (Ph), 932 (benzoxazine), 1274, 1072, 1010 (O=S=O) (S2).

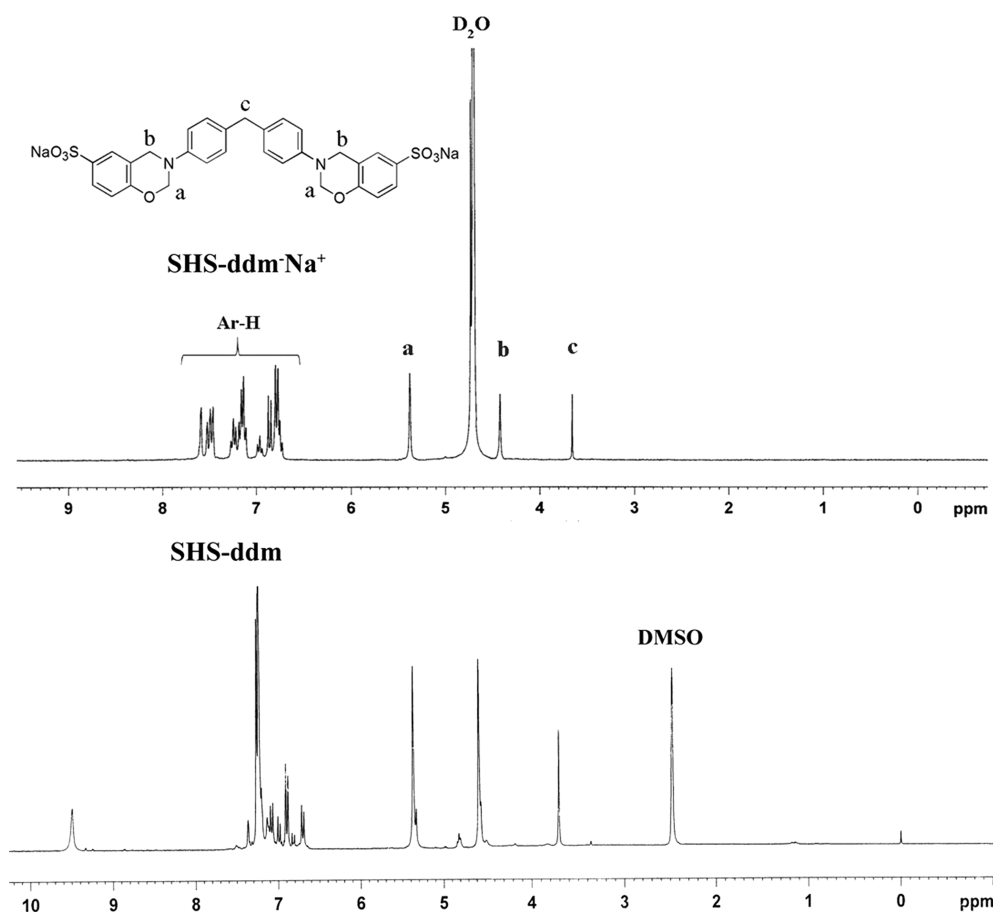
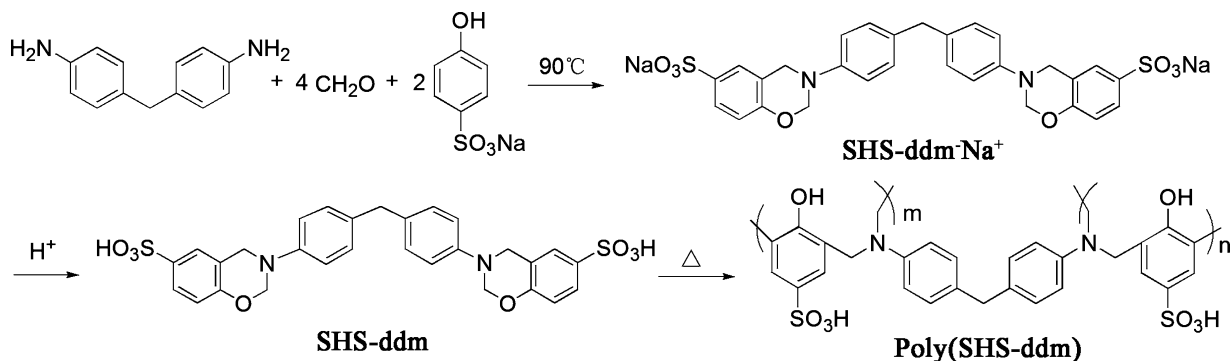
**Preparation of Sulfonic Acid-Containing Polybenzoxazine [poly(SHS-ddm)] Membrane.** Protonated monomer (SHS-ddm) was obtained by acidification of SHS-ddm<sup>−</sup>Na<sup>+</sup>. The SHS-ddm was dissolved in DMSO at a concentration of 20 wt %. An aliquot of 15 mL SHS-ddm solution was poured onto a clean PTFE dish (5 × 8 × 2 cm<sup>3</sup>). The cast membrane was allowed to dry at 120 °C for 4 h, followed by a programmed stepwise heating in an air-circulating oven as follows: 140 °C for 1 h, 160 °C for 1 h, 180 °C for 1 h, and 200 °C for 2 h. After being peeled from the substrate, the resulting cross-linked membrane was soaked in methanol and subsequently in deionized water at room temperature to remove any residual organic solvents. The polybenzoxazine membrane in the acid form was obtained with 100–150 μm thickness.

**Membrane Electrode Assembly (MEA) and Fuel Cell Test.** Catalyst layers of Pt/C (cathode) and Pt−Ru/C (anode) were

supported on carbon paper. The average Pt loadings of catalyst layer were 3.94 mg cm<sup>−2</sup> on the cathode and 4.20 mg cm<sup>−2</sup> on the anode. A 10 wt % Nafion solution was used as the binder for the Pt/C electrodes. The poly(SHS-ddm)-based MEA was assembled using a hot-press process. Two electrodes with effective areas of 1.00 cm<sup>2</sup> were hot-pressed onto both sides of a poly(SHS-ddm) membrane at 110 °C and 0.5 MPa for 195 s to form the MEA, which was mounted in a single cell fixture and installed in a lab-made fuel cell test station. For semipassive air-breathing direct methanol fuel cell (DMFCs) performance tests, methanol solutions with various concentrations (1–17 M) were supplied at a flow rate of 2 mL min<sup>−1</sup> and the air flow rate was 250 cm<sup>3</sup> min<sup>−1</sup>. Polarization curves were obtained over a temperature range from 40 to 80 °C. The durability tests of the single cell with poly(SHS-ddm) membrane was performed with 7 M methanol solution as the fuel at constant current density (200 mA cm<sup>−2</sup>).

**Characterization Methods.** <sup>1</sup>H NMR spectra were recorded on a 300 MHz UltraShield magnet spectrometer (Bruker), using D<sub>2</sub>O as the solvent. Fourier transform infrared (FTIR) spectroscopy was performed on a Bruker TENSOR27 spectrometer over a range of 4000 to 400 cm<sup>−1</sup> at a spectral resolution of 4 cm<sup>−1</sup>. Samples were prepared using the KBr pellet method. The electrospray ionization mass spectrometry (ESI-MS) spectra were obtained on an Agilent 6510 Q-TOF mass spectrometer for determining the molecular weight of the synthesized monomer, and the ionization power used was 70 eV. Differential scanning calorimetry (DSC) used a Mettler-Toledo DSC822e instrument at a heating rate of 10 °C min<sup>−1</sup> under a nitrogen atmosphere at a flow rate of 60 mL min<sup>−1</sup>. Dynamic mechanical analysis (DMA) was performed on Mettler-Toledo DMA/SDTA861e instrument at the frequency of 1 Hz in an oscillatory shear mode. A specimen with dimensions of approximately 5.00 mm × 4.00 mm × 0.600 mm was measured at a force amplitude of 0.5 N and a ramp rate of 3 °C min<sup>−1</sup> from 50 to 350 °C. Thermogravimetric analysis (TGA) was performed using a Mettler-Toledo TGA/ADTA851e thermal analyzer. The sample was dried under vacuum at 90 °C for 1 d, and then 6.0–10.0 mg of sample was heated from ambient temperature to 800 °C at a heating rate of 10 °C min<sup>−1</sup> under nitrogen. Mechanical property of the membrane was measured with a tensile tester AG-2000A (Shimadzu AUTO graph) at room temperature using a programmed cross-head speed of 50 mm min<sup>−1</sup>. The ion exchange capacity (IEC, mequiv of SO<sub>3</sub>H/g of dried polymer) of poly(SHS-ddm) and Nafion 117 was determined via titration using the following procedure: 0.1 g of membrane samples in the SO<sub>3</sub>H form was immersed in 50 mL of 2 M NaCl solution for 24 h, with stirring of the solution to convert the membrane from the H<sup>+</sup> to the Na<sup>+</sup> form completely. The NaCl/HCl solution was titrated against 0.01 M NaOH to an end point at pH 7.0 using methyl red as a pH indicator. Water uptake of the PEM was determined in wt % by placing sample into a constant humidity incubator for 24 h at room temperature, then rapidly wiping off the water on the surface and weighting the swollen PEM. Finally, wet PEM was dried in a vacuum oven at 70 °C for 24 h. Water uptake and dimensional stability of the membrane were evaluated by measuring the weight and dimensional changes of the membrane between dried and humidified state. The oxidative stability of the PEM was evaluated by Fenton's test as follows: A 1 × 1 cm<sup>2</sup> poly(SHS-ddm) membrane was first dried in vacuum oven at 60 °C for 12 h. The dried and preweighed membrane was soaked and stirred in Fenton's reagent (3% aqueous H<sub>2</sub>O<sub>2</sub> + 3 ppm FeSO<sub>4</sub>) at 80 °C for 1 h. Subsequently, it was immersed in deionized water to prevent further degradation. Oxidative stability was represented by weight loss (%) and physical appearance of the membrane. The hydrolytic stability was evaluated by immersing the poly(SHS-ddm) membrane into boiling deionized water for 1 week, while monitoring the proton conductivity value changes to determine their potential stability toward high temperature fuel cell environment. The methanol diffusion coefficient across the membrane was measured using a two-chamber liquid permeability cell. One 50 mL chamber contained 5 M methanol solution and the other 50 mL chamber was filled with deionized water. The methanol concentrations in the water cell were determined periodically using a GC-8A gas chromatograph (Shimadzu, Tokyo, Japan). The methanol permeability was calculated according to the

Scheme 1. Synthetic Route to SHS-ddm and Its Polymer

Figure 1.  $^1\text{H}$  NMR spectra of **SHS-ddm·Na<sup>+</sup>** and **SHS-ddm**.

following equation:  $C_B(t) = (A/V_B) \times (P/L) \times C_A \times (t - t_0)$  ( $L$  is the membrane thickness,  $A$  is the effective membrane area,  $C_A$  and  $C_B$  are the methanol concentrations in methanol and water chambers, respectively, and  $P$  is the methanol permeability). The proton conductivity of the PEM was measured by a four-point probe method using an impedance analyzer from 25 to  $100^\circ\text{C}$  under different relative humidity. The impedance of the sample film at the controlled humidity and temperature was measured using a Model 700D series electrochemical analyzer (CH Instruments) in the potentiostat mode with a perturbation amplitude of 20 mV over frequencies of 1 Hz to 20 kHz by the way of a Nyquist plot. Both the real ( $Z'$ ) and imaginary parts ( $Z''$ ) of the complex impedance in the membrane sample were simultaneously measured over a broad frequency range (1–20 kHz). When the imaginary component containing both the inductive reactance and the capacitive reactance approaches zero at higher frequency, the real  $Z'$ -axis intercept is close to the ohmic resistance

and can be considered as the ohmic resistance of the film sample, eliminating any effect of the resistance caused by the lead inductance and stray capacitance. Thus, the results were collected by Z-view and analyzed by the Z-plot software, and the polyelectrolyte resistance ( $R$ ) was determined from the high frequency intersection with the real axis in the impedance plot. When the impedance at a controlled humidity and temperature was accurately calculated, the corresponding proton conductivity can be calculated using

$$\sigma = d/RS \quad (1)$$

where  $d$  is the distance between the reference and sensing electrodes and  $S$  is the cross-sectional area of the membrane. Measurements were taken after equilibration at a controlled humidity and temperature for 2 h. At each relative humidity, the conductivity was measured several times to ensure the sample was fully equilibrated.

## RESULTS AND DISCUSSION

### Synthesis and Characterization of Poly(SHS-ddm).

Scheme 1 illustrated the preparation of sulfonic acid-containing benzoxazine monomer and its polymer. Sodium 4-hydroxybenzenesulfonate reacted with paraformaldehyde and 4,4'-diaminodiphenylmethane at a molar ratio of 2: 4: 1 to give SHS-ddm- $\text{Na}^+$  via Mannich reaction. Subsequently, protonated monomer (SHS-ddm) was obtained by acidification of the SHS-ddm- $\text{Na}^+$  by equimolar 1.0 M HCl solution. Finally, the cross-linked network of poly(SHS-ddm) was formed by polymerization at an elevated temperature.

Figure 1 showed the  $^1\text{H}$  NMR spectra of SHS-ddm- $\text{Na}^+$  and SHS-ddm. For SHS-ddm- $\text{Na}^+$ , the characteristic resonances at 5.38 and 4.41 ppm were assigned to methylene protons of  $-\text{O}-\text{CH}_2-\text{N}-$  and  $\text{Ar}-\text{CH}_2-\text{N}-$  in the oxazine ring, respectively. The resonance at  $\delta = 3.65$  ppm was assigned to the protons of methylene bridge in 4,4'-diaminodiphenylmethane. The integrated intensity ratio of these three resonances was 2.03: 2.00: 1.02, which was consistent with the theoretical value of 2.00: 2.00: 1.00. For SHS-ddm, the resonance at  $\delta = 9.56$  ppm was assigned to the hydroxy proton of the sulfonic group.

FTIR and ESI-MS spectra of SHS-ddm- $\text{Na}^+$  were shown in S1 and S2 in the Supporting Information, respectively. All experimental data from  $^1\text{H}$  NMR, FTIR, and ESI-MS analysis confirmed that the monomer was synthesized successfully.

Figure 2 showed the DSC thermograms of SHS-ddm- $\text{Na}^+$ , SHS-ddm, and poly(SHS-ddm). The exothermic peak of ring-

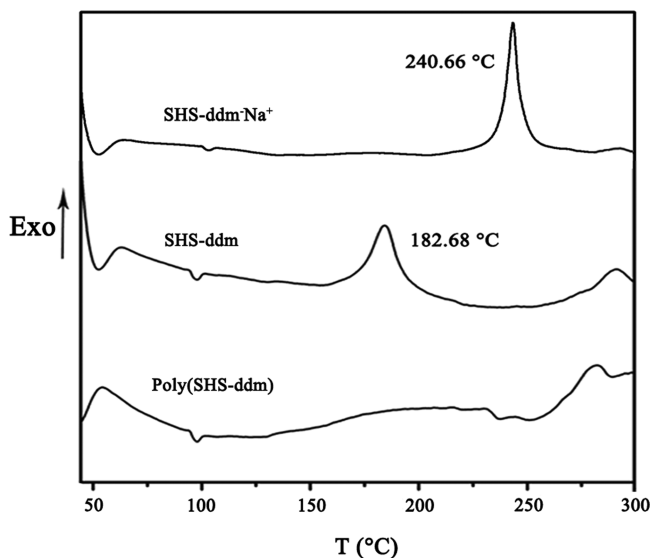


Figure 2. DSC thermograms of SHS-ddm- $\text{Na}^+$ , SHS-ddm, and poly(SHS-ddm).

opening polymerization was centered at 183 °C, which was lower than reported neutral benzoxazine monomer due to the existence of strong acid groups.<sup>18</sup> In addition, GPC measurement showed that a small peak at high molecular weight existed, which corresponded to the ring opened phenolic oligomer. It also caused the lower polymerization temperature. The onset and end exothermic temperatures were 162 and 205 °C, respectively. In order to determine whether the cross-linking reaction was completed, the DSC thermogram of cured sample was run. No obvious exothermic peak was observed

between temperatures of 160 and 210 °C, indicating that the ring-opening polymerization was complete.

The FTIR spectrum of poly(SHS-ddm) after polymerization at 200 °C for 2 h is shown in Figure S3 in the Supporting Information. The characteristic absorption band at 932  $\text{cm}^{-1}$  due to the benzene ring attached with oxazine disappeared completely. The band at 1508  $\text{cm}^{-1}$  due to trisubstituted benzene ring reduced its intensity. On the other hand, new absorption bands at 3240  $\text{cm}^{-1}$  due to phenolic hydroxyl group and at 1480  $\text{cm}^{-1}$  due to tetrasubstituted benzene ring appeared, suggesting that the polymerization of SHS-ddm occurred and afforded cross-linked polybenzoxazines.

Figure 3 showed the DMA curve of poly(SHS-ddm).  $T_g$  was observed at 245 and 225 °C from the maximum of  $\tan \delta$  and

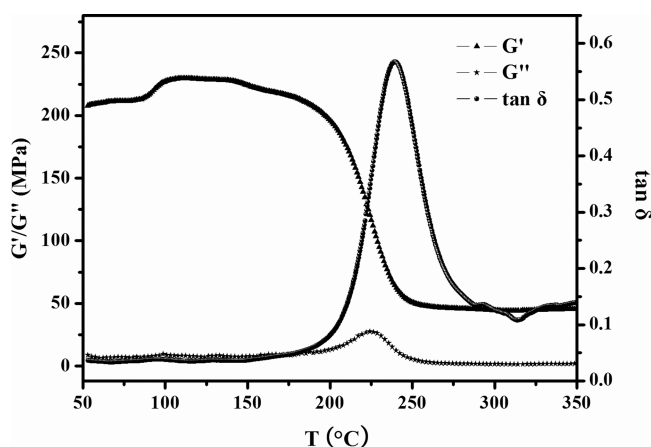


Figure 3. DMA curve of poly(SHS-ddm).

loss modulus  $G''$ , respectively. The high  $T_g$  of poly(SHS-ddm) was beneficial for use in high temperature fuel cells.

**Preparation and Characterization of the Proton Exchange Membrane.** Figure 4 showed a photograph of

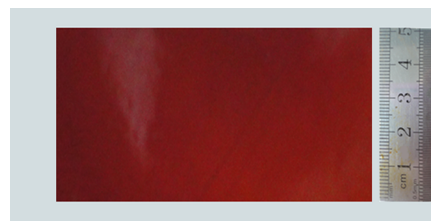
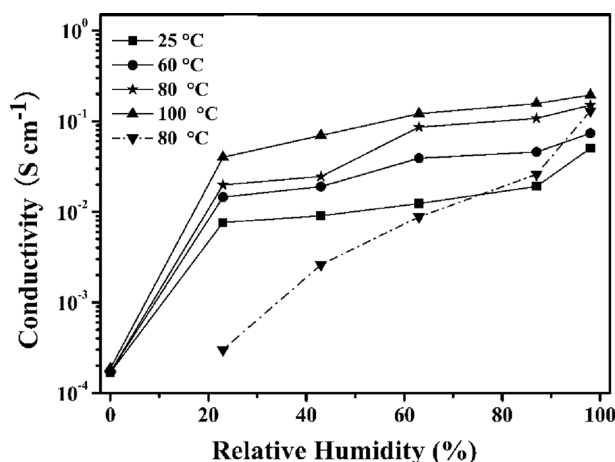


Figure 4. Photograph of the poly(SHS-ddm) membrane.

poly(SHS-ddm) membrane. The crimson poly(SHS-ddm) membrane (8 cm  $\times$  5 cm  $\times$  150  $\mu\text{m}$ ) was obtained through casting of the monomer solution and polymerization at elevated temperatures. The cast membrane was dried at 120 °C for 4 h to remove the solvent, followed by stepwise heating to complete the cross-linking reaction. The membrane was insoluble in water or common organic solvents such as dimethyl formamide (DMF), DMSO, *N*-methylpyrrolidone (NMP), and ethanol due to its cross-linked structure.

Figure 5 showed the proton conductivity of the poly(SHS-ddm) membrane as a function of relative humidity at different temperatures. For comparison, Nafion 117 was also measured under the same experimental conditions. The proton conductivity of poly(SHS-ddm) increased with increasing relative humidity and temperature. It reached 0.154  $\text{S cm}^{-1}$  at





**Figure 5.** Proton conductivity of the poly(SHS-ddm) membrane as a function of relative humidity at different temperatures (—, poly(SHS-ddm); ---, Nafion 117).

80 °C and 100% relative humidity(RH), which was close to that of Nafion 117. The value reached  $0.194 \text{ S cm}^{-1}$  at 100 °C while Nafion 117 had a significant loss in conductivity at this temperature due to the dehydration of water from the membrane. It should be noted that the conductivities of poly(SHS-ddm) membrane at low RH were much higher than that of Nafion 117. This might be caused by high contents of sulfonic acid groups in poly(SHS-ddm) (IEC = 3.13 mequiv/g) than Nafion 117 (IEC = 0.91 mequiv/g).

From conductivity–temperature relationship of the fully hydrated poly(SHS-ddm), the conductivity showed the Arrhenius-type behavior. The activation energy ( $E_a$ ) for proton conduction was calculated by the equation:  $\sigma = \sigma_0 \exp(-E_a/RT)$ , where  $R$  is the universal gas constant ( $8.314 \text{ J mol}^{-1} \text{ K}^{-1}$ ),  $T$  is the absolute temperature (K), and  $\sigma_0$  is the pre-exponential factor. The proton conduction in poly(SHS-ddm) membrane followed a proton-hopping dominant mechanism (or the Grotthuss mechanism) with an  $E_a$  value of  $12.69 \text{ kJ mol}^{-1}$  (see Figure S4 in the Supporting Information).

The methanol permeability, the selectivity parameter (SP), and mechanics data of poly(SHS-ddm) are listed in Table 1. The corresponding data of Nafion 117 and SPEEK under the same measurement conditions were also given for comparison. The methanol permeability of poly(SHS-ddm) membrane of was  $5.8 \times 10^{-8} \text{ cm}^2 \text{ s}^{-1}$ , which was near 2 orders of magnitude lower than that of Nafion 117 ( $1.98 \times 10^{-6} \text{ cm}^2 \text{ s}^{-1}$ ). This low methanol permeability was attributed to highly cross-linked network of poly(SHS-ddm).

Proton conductivity and methanol permeability are important factors influencing the DMFC performance. Both lower methanol permeability and higher proton conductivity are preferable. The ratio of the proton conductivity and methanol permeability ( $\sigma/P$ ) data, named selectivity parameter (SP), was

usually used as a token of methanol-resistant property.<sup>28,29</sup> The calculated SP value of poly(SHS-ddm) was  $2.655 \times 10^6 \text{ S s cm}^{-3}$ , which was much higher than that of Nafion 117 ( $8.081 \times 10^4 \text{ S s cm}^{-3}$ ). High SP value revealed that poly(SHS-ddm) membrane was particularly suitable for DMFCs. A moderate tensile strength of 32.5 MPa and an elongation at break of 15.1% were observed for wet poly(SHS-ddm) membrane with 20% water content.

Membrane stability was very important for PEMs. Fenton's test was often used to assess the stability of membranes toward the oxidative fuel cell operating conditions.<sup>30–33</sup> The original shape of poly(SHS-ddm) membrane was maintained over the testing course, and the oxidative weight loss percent [ $W(\text{ox})$ ] was only 1.2% for 1 h treatment with Fenton's reagent. These indicated high oxidative stability of the membrane (Table 2). The hydrolytic stability was evaluated by immersing the poly(SHS-ddm) membrane into boiling deionized water for 1 week. The nearly unchanged proton conductivities before ( $\delta_0 = 0.154 \text{ S cm}^{-1}$ ) and after ( $\delta_1 = 0.151 \text{ S cm}^{-1}$ ) the test revealed good hydrolytic stability. The water uptake values increased with increasing relative humidity, and reached 24.8% at 100% RH at room temperature. Both thickness and in-plane dimensional changes increased slightly with the largest value of 2.9% over the entire range of RH. The highly cross-linked polybenzoxazine matrix restricted the free volume of poly(SHS-ddm) and prevented excessive water swelling, resulting in moderate water uptake as well as admirable dimension stability. The 5% and 10% weight-loss temperatures were 304 and 345 °C, respectively. It suggested that poly(SHS-ddm) can meet the thermal stability requirement for PEMs in fuel cells.

**Fuel Cell Performance.** To minimize the efficiency reduce due to the methanol crossover in DMFC, the methanol concentration was usually lower than 2 M instead of the desired equimolar anode half-cell reaction concentration of 17 M.<sup>34–36</sup> However, if the problem of methanol crossover could be solved, a higher methanol concentration is strongly desirable due to higher specific energy and reduced cell weight. Therefore, the effect of fuel concentration on cell performance was evaluated in DMFC at 60 °C. Figure 6 showed the polarization curves of a DMFC single cell with various methanol concentrations at 60 °C. The maximum current density as a function of methanol concentration at constant cell voltage of 0.2 V was used to represent the cell performance.<sup>34</sup> It was clearly observed that the best methanol concentration was 7 M, and the maximum current density reached the highest value of  $328 \text{ mA cm}^{-2}$ . When the methanol concentration was over 7 M, the obtained maximum current density decreased with increasing methanol concentration. This was because that more methanol permeated through Poly(SHS-ddm) membrane and resulted in mixed potential and catalyst poisoning at the cathode.<sup>34,37–45</sup>

Figure 7 showed the polarization and power density curves of a DMFC single cell at various operating temperatures with a

**Table 1.** Comparison of Different PEM Properties

PEM	proton conductivity ( $\text{S cm}^{-1}$ ) <sup>a</sup>	methanol permeability $\times 10^6$ ( $\text{cm}^2 \text{ s}^{-1}$ )	SP values $\times 10^{-4}$ ( $\text{S s cm}^{-3}$ ) <sup>a</sup>	tensile strength (MPa)	elongation at break (%)
poly(SHS-ddm)	0.1540	0.058	265.5	32.49	15.11
Nafion 117	0.16	1.98	11.58	15	72
SPEEK	0.0168 <sup>b</sup>	0.145 <sup>b</sup>	8.081	57.32	20.28

<sup>a</sup>Proton conductivity measured at 80 °C and 100% relative humidity. <sup>b</sup>Tested for SPEEK with 47% sulfonation degree.<sup>26,27</sup>

Table 2. Oxidative, Hydrolytic, Dimensional, and Thermal Stability of Poly(SHS-ddm)

sample	oxidative stability $W(\text{ox})$ (%)	hydrolytic stability		dimensional change (%)	water uptake (%)	thermal stability	
		$\delta_0$ ( $\text{S cm}^{-1}$ )	$\delta_1$ ( $\text{S cm}^{-1}$ )			$T_{\text{ds}}$ ( $^{\circ}\text{C}$ )	$T_{\text{d10}}$ ( $^{\circ}\text{C}$ )
poly(SHS-ddm)	1.2	0.154	0.151	2.9	24.8	304	345

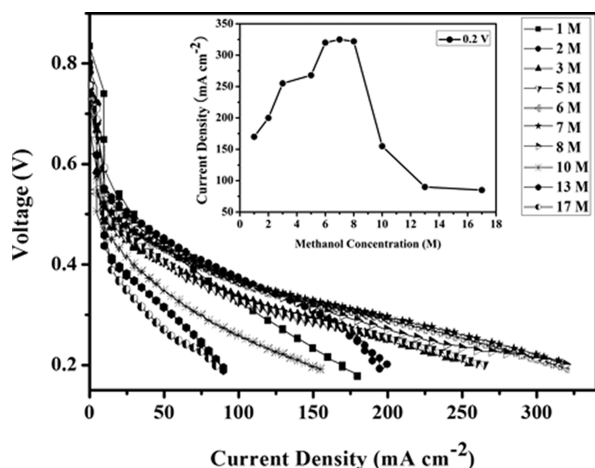


Figure 6. Polarization curves of a DMFC single cell with various methanol concentrations at 60 °C. The insert was fuel cell current density as a function of methanol concentration at constant cell voltage.

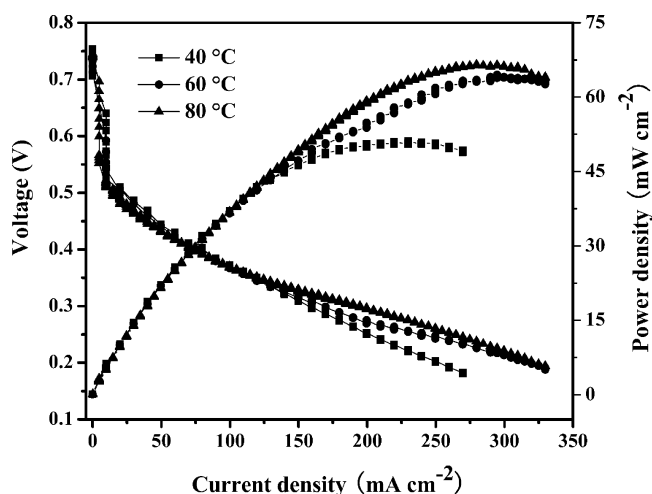


Figure 7. Polarization and power density curves of a DMFC single cell at various operating temperatures with a fixed methanol concentration of 7 M.

fixed methanol concentration of 7 M. The cell showed a stable open circuit voltage (OCV) of 0.76 V, indicating that the reactants were well separated by the poly(SHS-ddm) membrane. The initial voltage drop of polarization curve was mainly due to an electrochemical activation process, which was primarily caused by the sluggish kinetics of oxygen reduction at the cathode. The following linear decrease of polarization curve upon increasing current density was attributed to ohmic overpotential from the ion conduction through the electrolyte membrane and the electron conduction through electrode materials.<sup>46</sup> Maximum power output of a single cell increased with increasing cell temperature from 40 to 80 °C. At 80 °C, the cell showed a highest power density of 66.5  $\text{mW cm}^{-2}$ , and the maximum current density reached 330  $\text{mA cm}^{-2}$ . The increased output at higher temperatures was attributed to a

combination of factors consisting of a reduction of cell ohmic resistance, activation polarization, and concentration polarization.

Figure 8 showed the voltage decay during a stability test with a constant current density of 200  $\text{mA cm}^{-2}$  and a methanol

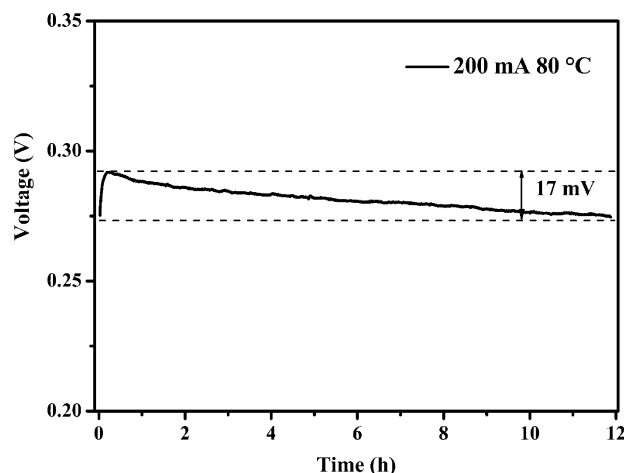


Figure 8. Stability test of a DMFC single cell with a constant current density of 200  $\text{mA cm}^{-2}$  at 80 °C for 12 h (methanol concentration: 7 M).

concentration of 7 M at 80 °C for 12 h. A relatively low voltage drop of 1.415  $\text{mV h}^{-1}$  from the initial value of 0.291 V was observed. The decay was probably caused by the agglomeration of electrocatalysts.<sup>47</sup> The optimizing of the conditions and exploring the reason for voltage decay is under investigation.

## CONCLUSIONS

In summary, a novel sulfonic acid-containing polybenzoxazine [Poly(SHS-ddm)] was successfully synthesized by ring-opening polymerization. Its cross-linked membrane was prepared through high temperature solution-casting method. The obtained poly(SHS-ddm) had high  $T_g$  (245 °C from  $\tan \delta$ ). The cross-linked poly(SHS-ddm) membrane exhibited a high proton conductivity of 0.154  $\text{S cm}^{-1}$  at 80 °C. We found its methanol permeability was  $5.8 \times 10^{-8} \text{ cm}^2 \text{ s}^{-1}$ . The calculated SP was  $2.655 \times 10^6 \text{ S s cm}^{-3}$ , which was much higher than that of Nafion 117 ( $8.081 \times 10^4 \text{ S s cm}^{-3}$ ). This value revealed that poly(SHS-ddm) membrane was particularly suitable for DMFCs. The poly(SHS-ddm) membrane also exhibited good oxidative, hydrolytic, and dimensional stability. Its tensile strength was 32.5 MPa, and the elongation at break was 15.1%. The performance of a DMFC single cell employing this membrane was evaluated. The results showed that the high methanol concentration up to 7 M can be used and its maximum attainable current density at 0.2 V reached the highest value of 328  $\text{mA cm}^{-2}$ . The cell exhibited a stable open circuit voltage of 0.76 V and a maximum power density of 66.5  $\text{mW cm}^{-2}$  at 80 °C. A low-voltage decay of 1.415  $\text{mV h}^{-1}$  using 7 M methanol as fuel was found after a continuous operation for 12 h. Overall, this novel polybenzoxazine exhibited special

potential for proton exchange membrane with low methanol permeability and low cost in direct methanol fuel cells.

## ■ ASSOCIATED CONTENT

### ■ Supporting Information

Detailed information about the FTIR and ESI–MS spectra of SHS-ddm<sup>−</sup>Na<sup>+</sup>, FTIR spectrum of poly(SHS-ddm), and regression curves of proton conductivity versus  $T^{-1}$ . This material is available free of charge via the Internet at <http://pubs.acs.org/>.

## ■ AUTHOR INFORMATION

### Corresponding Authors

\*(Z.L.) Telephone: +86-531-88361599. Fax: +86-531-88564464. E-mail: [z.lu@sdu.edu.cn](mailto:z.lu@sdu.edu.cn).

\*(L.Z.) Telephone: +01-216-368-5861. E-mail: [lxz121@case.edu](mailto:lxz121@case.edu).

### Notes

The authors declare no competing financial interest.

## ■ ACKNOWLEDGMENTS

We are thankful for the financial support from the National Natural Science Foundation of China (21074067). Z.L. also acknowledges support from the Chinese Scholar Council.

## ■ REFERENCES

- (1) Savadoga, O. J. *New Mater. Electrochem. Syst.* **1998**, *1*, 47–66.
- (2) Mauritz, K. A.; Moore, R. B. *Chem. Rev.* **2004**, *101*, 4535–4586.
- (3) Matsumoto, K.; Higashihara, T.; Ueda, M. *Macromolecules* **2009**, *42*, 1161–1166.
- (4) Hickner, M. A.; Ghassemi, H.; Kim, Y. S.; Einsla, B. R.; McGrath, J. E. *Chem. Rev.* **2004**, *104*, 4587–4611.
- (5) Hickner, M. A.; Pivovar, B. S. *Fuel Cells* **2005**, *5*, 213–229.
- (6) Zhang, H. W.; Shen, P. K. *Chem. Rev.* **2012**, *112*, 2780–2832.
- (7) Miyatake, K.; Yasuda, T.; Hirai, M.; Nanasawa, M.; Watanabe, M. *J. Polym. Sci., Part A: Polym. Chem.* **2007**, *45*, 157–163.
- (8) Chen, S.; Yin, Y.; Kita, H.; Okamoto, K. *J. Polym. Sci., Part A: Polym. Chem.* **2007**, *45*, 2797–2811.
- (9) Sutou, Y.; Yin, Y.; Hu, Z.; Chen, S.; Kita, H.; Okamoto, K.; Wang, H.; Kawasato, H. *J. Polym. Sci., Part A: Polym. Chem.* **2009**, *47*, 1463–1477.
- (10) Kang, S.; Zhang, C.; Xiao, G.; Yan, D.; Sun, G. *J. Membr. Sci.* **2009**, *334*, 91–100.
- (11) Li, N.; Zhang, S.; Liu, J.; Zhang, F. *Macromolecules* **2008**, *41*, 4165–4172.
- (12) Mader, J. A.; Benicewicz, B. C. *Macromolecules* **2010**, *43*, 6707–6715.
- (13) Xing, P. X.; Robertson, G. P.; Guiver, M. D.; Mikhailenko, S. D.; Kaliaguine, S. *Macromolecules* **2004**, *37*, 7960–7967.
- (14) Harrison, W. L.; Hickner, M. A.; Kim, Y. S.; McGrath, J. E. *Fuel Cells* **2005**, *5*, 201–212.
- (15) Miyatake, K.; Chikashige, Y.; Higuchi, E.; Watanabe, M. *J. Am. Chem. Soc.* **2007**, *129*, 3879–3887.
- (16) Gil, S. C.; Kim, J. C.; Ahn, D.; Jang, J. S.; Kim, H.; Jung, J. C.; Lim, S.; Jung, D. H.; Lee, W. *J. Membr. Sci.* **2012**, *417*–418, 2–9.
- (17) Ghosh, N. N.; Kiskan, B.; Yagci, Y. *Prog. Polym. Sci.* **2007**, *32*, 1344–1391.
- (18) Ning, X.; Ishida, H. *J. Polym. Sci., Part A: Polym. Chem.* **1994**, *32*, 1121–1129.
- (19) Ishida, H.; Sanders, D. P. *Macromolecules* **2000**, *33*, 8149–8157.
- (20) Choi, S.; Park, J.; Lee, W. Phosphorous containing benzoxazine-based monomer, polymer thereof, electrode for fuel cell including the same, electrolyte membrane for fuel cell including the same, and fuel cell employing the same. US 8,192,892 B2, Jun 5, 2012.
- (21) Choi, S.; Park, J. Naphthoxazine benzoxazine-based monomer, polymer thereof, electrode for fuel cell including the polymer, electrolyte membrane for fuel cell including the polymer, and fuel cell using the electrode. US 2012/0219876 A1, Aug 30, 2012.
- (22) Kim, S. K.; Ko, T.; Choi, S. W.; Park, J. O.; Kim, K. H.; Pak, C.; Chang, H.; Lee, J. C. *J. Mater. Chem.* **2012**, *22*, 7194–7205.
- (23) Kim, S. K.; Ko, T.; Kim, K.; Choi, S. W.; Park, J. O.; Kim, K. H.; Pak, C.; Chang, H.; Lee, J. C. *Macromol. Res.* **2012**, *20*, 1181–1190.
- (24) Kim, S. K.; Choi, S. W.; Jeon, W. S.; Park, J. O.; Ko, T.; Chang, H.; Lee, J. C. *Macromolecules* **2012**, *45*, 1438–1446.
- (25) Ye, Y. S.; Yen, Y. C.; Cheng, C. C.; Chen, W. Y.; Tsai, L. T.; Chang, F. C. *Polymer* **2009**, *50*, 3196–3203.
- (26) Li, L.; Zhang, J.; Wang, Y. X. *J. Membr. Sci.* **2003**, *226*, 159–167.
- (27) Li, X. F.; Liu, C. P.; Lu, H.; Zhao, C. J.; Wang, Z.; Xing, W.; Na, H. *J. Membr. Sci.* **2005**, *254*, 147–155.
- (28) Dashtimoghdam, E.; Hasani-Sadrabadi, M. M.; Moaddel, H. *Polym. Adv. Technol.* **2010**, *21*, 726–734.
- (29) Tohidian, M.; Ghaffarian, S. R.; Shakeri, S. E.; Dashtimoghdam, E.; Hasani-Sadrabadi, M. M. *J. Solid State Electrochem.* **2013**, *17*, 2123–2137.
- (30) Tang, H. L.; Pan, M.; Wang, Fang.; Shen, P. K.; Jiang, S. P. *J. Phys. Chem. B* **2007**, *30*, 8684–8690.
- (31) Wang, C. Y.; Li, N. W.; Shin, D. W.; Lee, S. Y.; Kang, N. R.; Lee, Y. M.; Guiver, M. D. *Macromolecules* **2011**, *44*, 7296–7306.
- (32) Lee, K. S.; Jeong, M. H.; Lee, J. P.; Lee, J. S. *Macromolecules* **2009**, *42*, 584–590.
- (33) Maity, S.; Jana, T. *Macromolecules* **2013**, *46*, 6814–6823.
- (34) Ge, J.; Liu, H. *J. Power Sources* **2005**, *142*, 56–69.
- (35) Elabd, Y. A.; Hickner, M. A. *Macromolecules* **2011**, *44*, 1–11.
- (36) DeLuca, N. W.; Elabd, Y. A. *J. Polym. Sci., Part B: Polym. Phys.* **2006**, *44*, 2201–2225.
- (37) Surampudi, S.; Narayanan, S. R.; Vamos, E.; Frank, H.; Halpert, G. *J. Power Sources* **1994**, *47*, 377–385.
- (38) Jung, D. H.; Lee, C. H.; Kim, C. S.; Shin, D. R. *J. Power Sources* **1998**, *71*, 169–173.
- (39) Abdolkareem, M. A.; Nakagawa, N. *J. Power Sources* **2006**, *162*, 114–123.
- (40) Han, J. H.; Liu, H. T. *J. Power Sources* **2007**, *164*, 166–173.
- (41) Scott, K.; Taama, W.; Cruickshank, J. J. *Appl. Electrochem.* **1998**, *28*, 289–297.
- (42) Elabd, Y. A.; Napadensky, E.; Sloan, J. M.; Crawford, D. M.; Walker, C. W. *J. Membr. Sci.* **2003**, *217*, 227–242.
- (43) Shaffer, C. E.; Wang, C. Y. *J. Power Sources* **2010**, *195*, 4185–4195.
- (44) Thangamuthu, R.; Lin, C. W. *Solid State Ionics* **2005**, *176*, 531–538.
- (45) Li, X. L.; Faghri, A.; Xu, C. *Int. J. Hydrogen Energy* **2010**, *35*, 8690–8698.
- (46) Chu, D.; Jiang, R.; Walker, C. J. *Appl. Electrochem.* **2000**, *30*, 365–370.
- (47) Liu, J. G.; Zhou, Z. H.; Zhao, X. S.; Xin, Q.; Sun, G. G.; Yi, B. L. *Phys. Chem. Chem. Phys.* **2004**, *6*, 134–137.